PRELIMINARY MEASUREMENT OF THE TRANSFER MATRIX OF A TESLA-TYPE CAVITY AT FAST*

A. Halavanau[1,2], N. Eddy[2], D. Edstrom[2], A. Lunin[2], P. Piot[1,2], J. Ruan[2], J. Santucci[2], N. Solyak[2]
[1] Department of Physics and Northern Illinois Center for Accelerator & Detector Development, Northern Illinois University, DeKalb, IL 60115, USA
[2] Fermi National Accelerator Laboratory, Batavia, IL 60510, USA

Abstract

Superconducting linacs are capable of producing intense, ultra-stable, high-quality electron beams that have widespread applications in Science and Industry. Many current and planned projects employ 1.3-GHz 9-cell superconducting cavities of the TESLA design. In this paper we discuss the transverse-focusing properties of such a cavity and non-ideal transverse-map effects introduced by field asymmetries in the vicinity of the input and high-order-mode radiofrequency (RF) couplers. Specifically, we consider the case of a cavity located downstream of an RF-gun in a setup similar to the photoinjector of the Fermilab Accelerator Science and Technology (FAST) facility. Preliminary experimental measurements of a cavity transverse matrix were carried out at the FAST facility. The results are discussed and compared with analytical and numerical simulations.

CAVITY MODELS

Several proposed or operating accelerator facilities include standing-wave (SW) TESLA-type cavities [1], to accelerate electron, muon, or proton beams, e.g. [2–4]. The transverse beam dynamics associated to these accelerating cavities plays a crucial role and has been the object of several studies [5–7]. The transfer matrix of a π-mode RF resonator was derived by Chambers [8] and later generalized to accelerating field with spatial harmonics [9–11].

The Chambers Model can be derived by considering the transverse motion of the particle in a standing wave RF field $E_z(z,t) = E_0 \sum_n a_n \cos(nkz)\sin(\omega t + \Delta\phi)$, where E_0 is the average accelerating gradient, k is the wave number associated with n-th harmonic of amplitude a_n, $\Delta\phi$ is the phase advance of the particle and z is the longitudinal coordinate along the cavity axis.

The ponderomotive-focusing force is obtained under the paraxial approximation as $F_r = -e(E_r - vB_\phi) \approx er\frac{\partial E_z}{\partial z}$ where $v \simeq c$ is the particle velocity along the axial direction. Using the identity $(1 \pm n)\cos(x)\sin[y(1 \pm ny)] + (1 \pm n)\sin(x)\cos[y(1 \pm n)] = (1 \pm n)\sin[(1 \pm n)y \pm x]$, ref. [11] shows that the force averaged over one RF-period in the first order of perturbation theory yields the focusing strength, $\bar{K}_r = -\frac{(E_0 e)^2}{8(\gamma m)^2}$, for the case of a "pure" standing wave resonator. The equation of motion then takes form:

$$x'' + \left(\frac{\gamma'}{\gamma}\right)x' + \bar{K}_r\left(\frac{\gamma'}{\gamma}\right)^2 x = 0, \tag{1}$$

where x is the transverse coordinate, $x' \equiv \frac{dx}{ds}$, $\gamma' \equiv \frac{d\gamma}{ds} = eE_0\cos(\Delta\phi)/m_0c^2 \equiv \bar{G}_{rf}/m_0c^2$ is the normalized energy gradient (γ is the Lorentz factor). The solution of the Eq. (1) is of the form $\mathbf{x}_f = R\mathbf{x}_i$ where $\mathbf{x} \equiv (x, x')$ and the subscript i (resp. f) corresponds to the coordinates upstream (resp. downstream) of the cavity. The 2×2 matrix R is given by [8]

$$\begin{aligned}
R_{11} &= \cos\alpha - \sqrt{2}\cos(\Delta\phi)\sin\alpha,\\
R_{12} &= \sqrt{8}\frac{\gamma_i}{\gamma'}\cos(\Delta\phi)\sin\alpha,\\
R_{21} &= -\frac{\gamma'}{\gamma_f}\left[\frac{\cos(\Delta\phi)}{\sqrt{2}} + \frac{1}{\sqrt{8}\cos(\Delta\phi)}\right]\sin\alpha,\\
R_{22} &= \frac{\gamma_i}{\gamma_f}[\cos\alpha + \sqrt{2}\cos(\Delta\phi)\sin\alpha],
\end{aligned} \tag{2}$$

where $\alpha \equiv \frac{1}{\sqrt{8}\cos(\Delta\phi)}\ln\frac{\gamma_f}{\gamma_i}$, and $\gamma_f \equiv \gamma_i + \gamma' z$ is the final Lorentz factor.

An alternative way of solving Eq. (1) in a piecewise fashion was formulated in [12]. This semi-analytical method can accommodate arbitrary spatial axial-field profiles.

Note, that the analytical solution of Eq. (1) is obtained under the assumption of axially symmetric field; it is not the case in a real RF cavity which includes input-power and high-order-mode (HOM) couplers needed to respectively couple the RF power to the cavity and damp the HOM fields excited by the beam.

To investigate the impact of couplers further, a 3D electromagnetic model of the cavity − including its auxiliary couplers − was implemented in HFSS [13]. The simulated 3D field map was imported in ASTRA [14] particle-tracking program. Figure 1 compares the evolution of beam centroid and envelope with and without including 3D effect in the cavity. For the 1D case (i.e. without including 3D effect) ASTRA uses the axial E field $E_z(z)$ derived from the 3D map and performed a paraxial expansion of for radial $E_r(z)$ and azimuthal $B_\theta(z)$ fields. The main impact of the HOM and input coupler is a slight beam steering. For our beam parameters, it was found that the transverse emittance was not significantly affected when the 3D field map was used.

* This work was supported by the US Department of Energy under contract DE-SC0011831 with Northern Illinois University. Fermilab is operated by the Fermi research alliance LLC under US DOE contract DE-AC02-07CH11359.

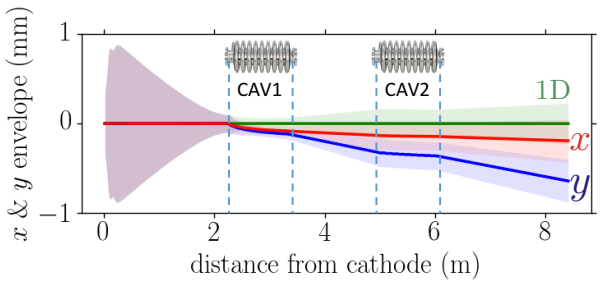

Figure 1: Evolution of beam centroid (solid traces) for the paraxial model (green) and the model including the 3D electromagnetic model of the cavity (the red and blue traces respectively correspond to horizontal and vertical position). The shaded area indicates the extent of the rms beam envelope. The simulation was carried out for a 5 MeV 20-pC bunch.

EXPERIMENTAL SETUP & METHOD

The preliminary experiment was performed at the FAST injector [15]. The 5-MeV beam formed in an RF gun was injected in a TESLA cavity (with average accelerating gradient limited to $\bar{G}_{rf} \simeq 17$ MeV/m and accelerated to a maximum energy of ~ 22 MeV; see Fig. 1 (note that CAV1 has been installed since the test was first performed; comparison to simulations is shown in Fig. 1). Pairs of electromagnetic button-style beam position monitors (BPMs) located up- and downstream of the cavity respectively provide input $\mathbf{X_i}$ and final $\mathbf{X_f}$ beam positions and divergences [here $\mathbf{X} \equiv (x, x')^T$].

Correspondingly, given the transfer matrix of the cavity R, we have $\mathbf{X_f} = R\mathbf{X_i}$. Consider $\mathbf{X_{0_i}}$ to be some reference orbit, so that we can rewrite the transformation as $\mathbf{X_f} = R(\mathbf{X_{0_i}} + \Delta\mathbf{X_{0_i}})$. It immediately follows that $R(\mathbf{X_{0_i}} + \Delta\mathbf{X_{0_i}}) = \mathbf{X_{0_f}} + \Delta\mathbf{X_{0_f}}$ and therefore $\Delta\mathbf{X_{0_f}} = R\Delta\mathbf{X_{0_i}}$. So any selected orbit can serve as a reference orbit to find the transformation R, assuming the set of perturbed trajectories around this reference are transformed linearly (which is the essence of the paraxial approximation).

In fact, once a set of perturbations is applied one can prove that the averaged orbit can be used as a reference orbit. The reference orbits method therefore mitigates the physical displacement of the BPMs along the beamline. Given a set of perturbation in initial coordinates $\Delta\mathbf{X_{i,n}}$ (where $n = 1, ..., N$ is an integer), the final coordinates downstream of the cavity are $\Delta\mathbf{X_{f,n}} = R\Delta\mathbf{X_{i,n}}$. Impressing a set of N perturbations results in a system of N equations of the form $\Xi_f = R\Xi_i$ where Ξ_j $(j = i, f)$ are $2 \times N$ matrices containing the positions and divergence associated to the N perturbations. This system is inverted via a least-square technique to recover R. The method can be further extended to the transverse 4D phase space to yield the 4×4 transfer matrix of the cavity.

The beam-trajectory perturbations are applied via small kicks from beam horizontal and vertical steerers located upstream of the cavity. In our experiment kicks were randomly applied to uniformly populate the transverse (x, x', y, y') trace space while monitoring the transmitted charge to ensure no beam loss occured.

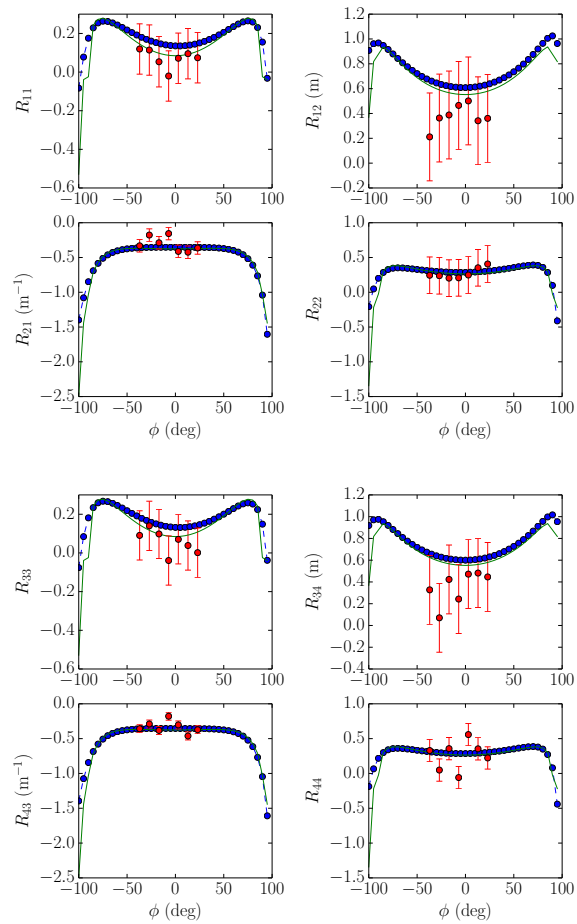

Figure 2: Main diagonal block of the transport matrix. The solid (green) lines represent Chambers' approximation, dashed (blue) lines with round markers are obtained from 3D field map simulations, and circular markers correspond to experimental values.

RESULTS

The measurements were made for 7 phases in a range of [-37,23] degrees. Each time ~ 800 trajectories were recorded corresponding to 200 different orbit settings recorded 4 times to average over possible beam-position jitter and provide statistical error bars. The comparison of the recovered transfer matrix element with the Chambers' model and the one derived from particle tracking with ASTRA in the 3D field map are presented in Figs. 2, 3, and 4.

First, it should be noted that the slight discrepancies between the Chambers' model and the particle tracking results are attributed to the non-ultra-relativistic nature of the beam upstream of the cavity [16].

Overall we find some agreement between experiment and models for the 2×2 diagnonal blocks of the experimen-

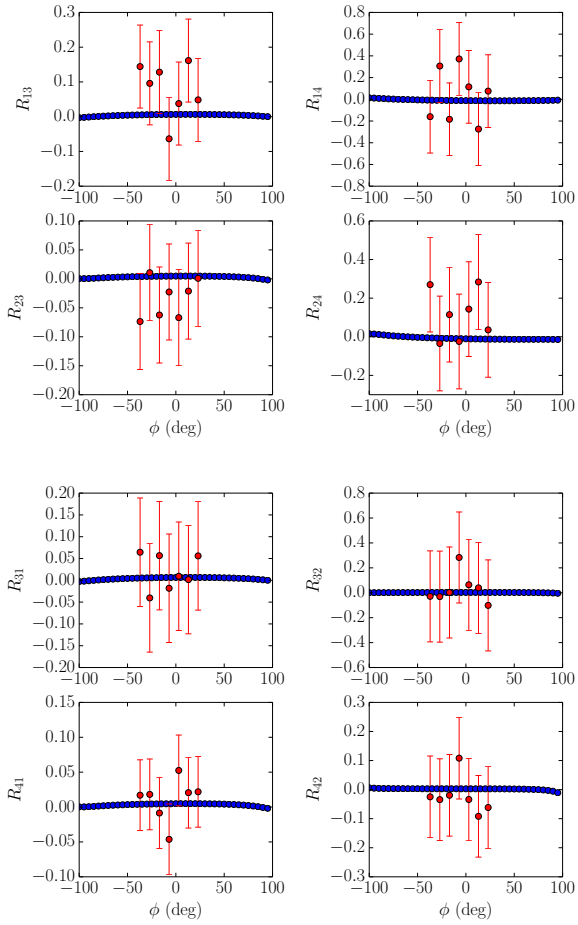

Figure 3: Anti diagonal block of the transport matrix. Lines and markers are as in Fig. 2.

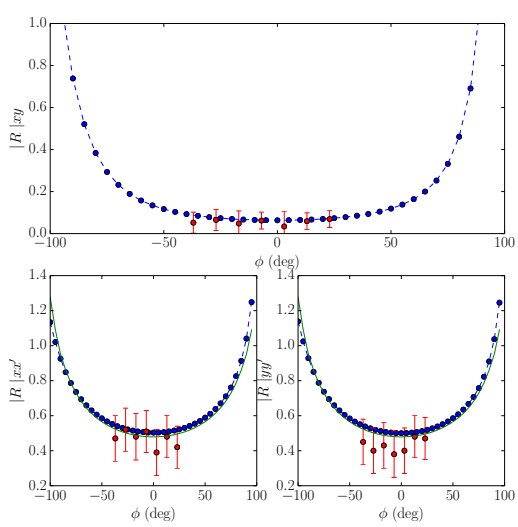

Figure 4: Transfer matrix determinant, calculated for full 4×4 matrix (top) and main diagonal block matrices determinants shown in Fig. 2.

tal transfer matrix; see Fig. 2. Some elements, e.g. R_{12} have larger discrepancies but our error bars for the present measurement are significant.

The coupling (anti-diagonal) 2×2 blocks modeled by the simulation are very small and seem to be corroborated with our experimental results, albeit for the large error bars; see Fig. 3. The latter observation indicates that for the range of parameters being explored the 3D effects associated to the presence of the couplers appear to have a very small effect on the beam dynamics. Finally, we find that determinant $|R|$ is consistent within the error bars with simulations; see also [6].

SUMMARY

We reported our progress toward the measurement of the transfer matrix of a TESLA-type cavity at FAST. Despite some technical limitations, the presented measurements are consistent with the results from 3D field map simulations. Further improvements in the experimental setup were implemented and a refined measurement is planned in the near future.

REFERENCES

[1] B. Aunes, et al. Phys. Rev. ST Accel. Beams **3**, 092001(2000).

[2] A. Vivoli, et.al., technical note LCLS-II TN-15-03 (2015).

[3] M. Popovic and R.P. Johnson, Nucl. Phys. Proc. Suppl., **155**, 305, (2006).

[4] S. Holmes, et. al., Proc. of IPAC2015, THPF116, (2015).

[5] S. Reiche, et. al., Phys. Rev., **E56**, 3572 (1997).

[6] P. Piot and Y.E. Sun. Report Beams Document 1521-v1, Fermilab (2004).

[7] P. Piot, et. al., Conf. Proc., C0505161:4135 (2005).

[8] E.E. Chambers. HEPL TN-68-17 and HEPL 570 (Oct. 1968).

[9] J. Rosenzweig and L. Serafini. Phys. Rev., **E49**, 1599 (1994).

[10] S. C. Hartman and J. B. Rosenzweig. Phys. Rev., **E47**, 2031 (1993).

[11] S.C. Hartman. Phd thesis. *UCLA* (1994).

[12] Yu. Eidelman, *et. al.*, Conf. Proc., C110328:1725 (2011).

[13] High Frequency Structure Simulator software available from ANSYS.

[14] K. Flöttmann. *ASTRA reference manual*, DESY (2000).

[15] E. Harms, et al., ICFA Beam Dyn. Newslett., **64** 133 (2014).

[16] S. Fartoukh Report TESLA 98-01, DESY (1998).